SUPPRESSION OF VORTEX CORE PRECESSION IN A STRONGLY SWIRLING LIFTED FLAME BY HIGH-AMPLITUDE AXIAL FORCING

S.V. Alekseenko[1,2], V.M. Dulin[1,2]*, Yu.S. Kozorezov[1], D.M. Markovich[1,2]
*: vmd@itp.nsc.ru
1: Institute of Thermophysics, Siberian Branch of RAS, 1 Lavrentyev Avenue, Novosibirsk, 630090, Russia
2: Department of Physics, Novosibirsk State University, 2 Pirogova Street, Novosibirsk, 630090, Russia

Abstract
The present work describes the effect of axial forcing on a swirling lifted propane-air flame. Stereo Particle Image Velocimetry technique was used to estimate instantaneous velocity and vorticity fields in the reacting and isothermal swirling flows with and without forcing. The spatial distributions of the average velocity and components of turbulent kinetic energy were calculated for the measured ensembles of the instantaneous fields. The used swirler provided flows with a pronounced vortex breakdown and bubble-type recirculation zone both for the reacting and isothermal conditions. The axial forcing with relatively large amplitude was observed to significantly affect the lifted flame structure by modifying large-scale vortices. The paper demonstrates that the forcing provided an increase of turbulent combustion rate and suppressed precession of the vortex core near the burner exit. It was concluded that interaction of the lifted flame with forced large-scale vortices resulted in this effect.

Introduction
The application of a swirl is often used for stabilization of jet flames via increasing turbulent fluctuations upstream the flame front and by providing a low-velocity region or recirculation zone (for low or high swirl rates, respectively) near the burner exit [8], [15], [3]. Therefore, the flow swirling can provide stable lean combustion regimes of premixed flames at a wide range of flow rates and can be used to reduce NOx formation. Thus, the swirl application can be considered as an efficient way to passively control flow structure of jets and flames. However, even for isothermal swirling jets, substantially different flow regimes can be observed, depending on the swirl rate and the manner in which the swirl is applied (e.g., [16]). It has been widely acknowledged by many authors that Kelvin–Helmholtz instability leading to vortex rings formation dominates in the shear layer of non-swirling and weakly swirling jets. For a sufficiently high swirl rate (but before the appearance of a pronounced vortex breakdown, VB), strong helical waves dominate the mixing layer of the jet. A further increase in the swirl rate leads to the breakdown of the swirling jets' vortex core, which has been observed in different states: spiral, bubble, and conical, where the latter two can be either symmetric or asymmetric. From a number of experimental, theoretical and numerical studies on the criterion for VB, it can be inferred that the breakdown usually appears in a jet flow when the integral swirl rate S (defined as the ratio of the axial flux of angular momentum to the product of the axial flux of axial momentum and the radius) exceeds a critical value in the range of 0.5-0.8 (e.g., [4], [16], [18]). Based on the literature, it can be outlined that the flow structure of the strongly swirling jets with bubble-type VB and precession of the vortex core manifests some common features, even for rather different nozzle geometries. Recent studies [19], [16] indicate that precession of the vortex core in a strongly swirling jet is the result of the global helical instability mode $|m| = 1$ growth in an absolutely unstable jet flow with an initially axisymmetric recirculation zone (RZ), while the RZ appears near the nozzle exit

when the swirling jet column becomes centrifugally unstable after sudden expansion of the flow. In an experimental study of an isothermal swirling free jet at a low Reynolds number (Re = 1,000) and various swirl rates, [16] showed that after the VB, strong helical modes m = +1 and +2 coexisted in the flow and that m = +1 had the largest amplitude. The measurements showed that when the RZ appeared, the m = +1 oscillation first dominated the inner shear layer between the central RZ and the mean flow and then affected the outer shear layer between the jet and the ambient fluid. For a turbulent strongly swirling jet the authors [6] showed that 3D spatial structure of coherent vortices corresponded to a couple of secondary helical vortices (one vortex was located inside the RZ and the other outside, in the outer mixing layer) which were induced by the precession of the vortex core. Obviously, the presence of combustion makes the structure of the swirling jets much more complex, because of gas expansion and buoyancy effects [18], a combustion-induced VB phenomenon (e.g., [13]), etc. For example, the presence of combustion is known to suppress the vortex core precession in strongly swirling jets [3] and also to affect it weakly [4].

Another well-known efficient way to control turbulent structure (formation and downstream evolution of vortices) of non-swirling jet flows is the periodical excitation of the initial velocity (e.g., [5]). In particular, the excitation strongly affects stabilization height of a lifted non-swirling flame via altering ring-like vortices developing in the jet shear layer upstream the flame [7], [17]. Periodic forcing is also can be used to control the development of large-scale vortices and turbulent mixing in weakly [10] and even in strongly [1] swirling isothermal jets. Based on Large Eddy Simulation of a lean swirling flame in a model combustor, [12] have showed that application of periodic forcing with frequencies below the precession frequency of the vortex core can results in weakening the core precession and consequently shifts RZ and combustion domain upstream the combustor. On the basis of experimental and numerical data for premixed swirling flame in a model combustor (the swirl rate was about 0.55) [19] concluded that the swirling flame response to periodic forcing was governed by two main mechanisms: variation of the swirl rate and roll-up of the large-scale vortices. Depending on the forcing frequency, confluence of these mechanisms can result in a high or low level of heat release fluctuations. It is also suitable to note here that small flap actuators can be efficiently used to control vortices formation and mixing in a non-swirling jet [22] and weakly swirling jet [21]. In particular, the actuators can be also utilized to control stabilization of a lifted diffusion flame [14].

The present paper aims on the experimental study of a rich strongly swirling lifted flame under high-amplitude forcing of the initial velocity, since a significant forcing effect on the flame was recently documented [2]. The modification of turbulent reacting and isothermal flows (at the same inflow conditions) was investigated by means of stereo Particle Image Velocimetry (PIV). CH* chemiluminescence imaging was also applied to visualize region of turbulent combustion for the reacting case.

Experimental setup and apparatus

The measurements were performed in a combustion rig consisted of a burner, air fan, plenum chamber, flow seeding device, premixing chamber and section for the air and fuel (propane) flowrate control. The experiments were performed at atmospheric pressure. The burner represented a contraction nozzle with a swirler mounted inside. The nozzle exit diameter d was 15 mm. The swirl rate based on geometry of the swirler corresponded to $S = 1.0$. The nozzle had the same geometry as in the previous studies of swirling jets and flames [1], [2], [3]. It produced a strongly swirling jet flow with a pronounced VB and bubble-type RZ. During the present PIV study of the reacting flow, Re_{air} number (based on the nozzle exit diameter d, mean flowrate velocity and viscosity of the air) was 4,100. The equivalence ratio Φ of air-propane mixture issuing from the burner was 2.5. These parameters provided a

strongly swirling lifted flame with flow structure resembling to that for the isothermal flow [3]. In both isothermal and reacting cases, a precession of the vortex core was observed, and the coherent vortex structures were similar to the helical vortices reported by [6]. For the external periodical forcing of the flow, a system consisting of four loud speakers (a similar system was used by [5]), connected to an amplifier, function generator and electric power meter, was used. The normalized (by nozzle exit diameter d and the mean flowrate velocity U_0 of the mixture) forcing frequency, i.e., the Strouhal number St, was varied from 0.1 to 3. The forcing amplitude was calibrated by a Laser Doppler Velocimetry probe for various frequencies and ac power of sine voltage applied to the system of loud speakers. The referred amplitude of forcing a_f was defined as the intensity of the longitudinal velocity fluctuations at exit of the nozzle without swirler.

For the instantaneous velocity measurements, a "PIV-IT" Stereo PIV system consisting of a double-cavity 70 mJ Nd:YAG pulsed laser, couple of 4M CCD cameras and a synchronizing processor was used. The laser sheet formed by the system of lenses had a minimal thickness of 0.8 mm in the measurement section. In order to provide PIV measurements, the main flow, issuing from the nozzle, was seeded by TiO_2 particles with the average diameter of 1 μm. The ambient air was seeded by using a fog generator. The cameras were equipped with narrow-bandwidth optical filters admitting the emission of the laser (532 nm) and suppressing the radiation of the flame. The system was operated by a computer with "ActualFlow" software. The captured PIV images were processed by an iterative cross-correlation algorithm with an image deformation, a final interrogation area size of 32×32 pixels, and 50% overlap. Due to a non-uniform seeding of the tracer particles on the flow, the cross-correlation algorithm used was modified to account for the number of particles present in each interrogation area. The identification of the particles was done by Particle Mask Correlation method ([11], [23]) suitable for even a high particle concentration. Calculated instantaneous velocity vectors were validated using a signal-to-noise criterion for cross-correlation maxima and by the adaptive median filter proposed by [24]. Stereo calibration was performed by using a multi-level calibration target and a 3rd-order polynomial transform. The target of 150×150 mm^2 size had three levels of calibration markers: {–2, 0, +2} mm. In addition, to minimise the stereo calibration error, an iterative correction procedure of possible misalignment of the laser sheet and target plane was applied. The PIV measurements were performed in a central plane of the jet/flame. For each combustion regime, 1,500 instantaneous three-component velocity fields were measured. Based on the estimated instantaneous velocity fields, the spatial distributions of the mean velocity and components of turbulent kinetic energy (TKE) were calculated. To investigate the spatial structure of large-scale vortices emerging in the studied flows, a second-order centred difference scheme was used to calculate instantaneous vorticity fields. It should be mentioned that the scheme used is a low-pass derivative filter with a transfer function similar to that of the cross-correlation operator in the case of a 50% interrogation area overlap. Thus, the distributions of the instantaneous vorticity and the velocity shown below correspond only to large-scale fluctuations (greater than 1.1 mm).

For the analysis of spatial domain of turbulent combustion, CH* chemiluminescence signal from the swirling flames was captured by an UV-sensitive 1.5 Mpix ICCD camera equipped with a band-pass optical filter (430±5 nm). To allow comparison between the unforced and forced cases, the exposure duration (100 μs) and aperture of the lens used (set to the smallest value) were fixed. The chemiluminescence of other radicals admitted by the filter was assumed to be small, at least for the flame front. Nevertheless, the CO_2 emissions in the range 425-435 nm [9] could be significant in some regions. Five hundred 10-bit images of CH* chemiluminescence were captured, converted to floating point data, and then averaged

for each combustion regime. For analysis of the spatial structure of turbulent combustion region, an inverse discrete Abel transform (A^{-1}) was applied to the average images.

Results

Flame visualization

Figure 1 shows a Re-Φ diagram with the regions of typical combustion regimes and a blow-off curve for the strongly swirling flame. The blow-off curve corresponds to the flame parameters preceding the flame blow-off by the upstream flow when the flow rate of the air was increased. There is also a lower limit that corresponds to a flash-back of the flame inside the burner. The domain between the blow-off and flash-back limits in the Re-Φ diagram can be divided into three main regions of typical combustion regimes: attached flames with the front anchored to the nozzle rim; quasi-tubular flames with the front penetrating inside the nozzle; and lifted flames, which were typical for high Re_{air} and rich mixtures. In general, the strongly swirling turbulent (for Re_{air} typically above 2 000) flame was stabilised inside the RZ (as the quasi-tubular regime) when Φ was in the range close to flammability limits for a homogenous propane-air mixture at normal conditions (e.g., $0.6 < \Phi < 2.3$ for $Re_{air} = 4\,000$). If Φ was smaller, the flame was blown away; if Φ was higher, the combustion occurred as the lifted flame after the mixing of the main flow issued from the nozzle with the ambient air. From the examples in Figure 1b and Figure 2a, one can observe that the lifted flame represented a domain of intensive turbulent combustion located less than one d downstream the nozzle exit. Also, since the mixture coming from the nozzle was relatively rich ($\Phi = 2.5$) an extensive region of products afterburning was present further downstream, where soot luminescence was observed. Figure 2b and c demonstrates the most pronounced effect of the axial velocity forcing (among tested frequencies and amplitudes) on the strongly swirling lifted flame. The considered forcing frequency 170 Hz corresponded to the Strouhal number of $St = 0.6$. For this frequency and amplitude a_f approximately above 25% of U_0, a considerable modification of lifted flame was observed. In particular, a less soot luminosity can be seen above the domain of intensive turbulent combustion. It was concluded to be caused by an enhancement of turbulent heat and mass transfer in the initial region of the flow near the burner exit due to the strong forcing.

The average flow structure

The integral (on the line-of-sight through the flame) images of CH* chemiluminescence, averaged over 500 samples, are shown in Figure 3 (in pseudo colour) for the unforced and forced ($St = 0.6$) lifted flames. Analysis of the mean chemiluminescence distributions reveals that the high amplitude periodic forcing led to an increase in overall combustion intensity in the initial region of the lifted flame. The domain of turbulent combustion also slightly moved downstream and became wider. Figure 4 shows the spatial distributions of the mean velocity for the strongly swirling lifted turbulent flames. Length of the vectors shows the in-plane magnitude, while their colour scale corresponds to the magnitude of three-component vectors. The figure also contains the reconstructed average CH* chemiluminescence source. In all cases, a bubble-type VB took place and the main flow issued from the nozzle as an annular jet with a certain opening angle. The flow propagated around the RZ located at the jet axis (shown by a red heavy line in Figure 4). A monotonous decrease of the RZ longitudinal size with the forcing amplitude can be seen, wile the lateral size was almost constant (around $0.65d$). As can be seen, the intensive combustion domain slightly shifted downstream and become wider when the forcing was applied. In this domain, an increase of the gas velocity magnitude and growth of the jet spreading rate can be seen, and the fluid expansion augmented with a_f. This is considered to be caused by an intensification of turbulent combustion near the burner exit.

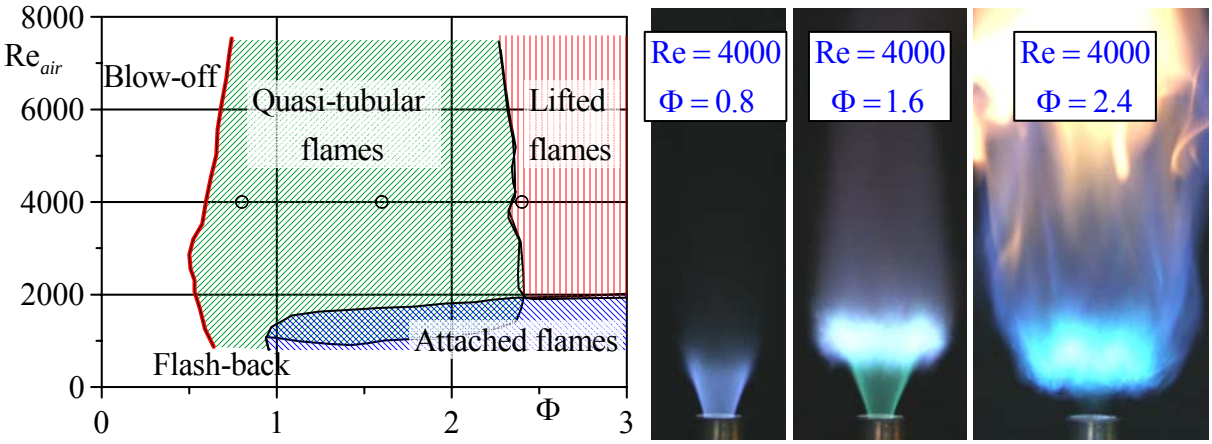

(a) (b)

Figure 1. (a) Re-Φ diagram with typical combustion regimes and blow-off limit (red heavy line) for a strongly swirling flame (S = 1.0). (b) Direct images of typical combustion regimes for Re_{air} = 4 000.

(a) (b) (c)

Figure 2. Direct images of a lifted strongly swirling flame (a) without periodic forcing and under forcing with St = 0.6: (b) a_f/U_0 = 20%, (c) a_f/U_0 = 30%. S = 1.0, Re_{air} = 4 100, Φ = 2.5, U_0 = 4.7 m/s

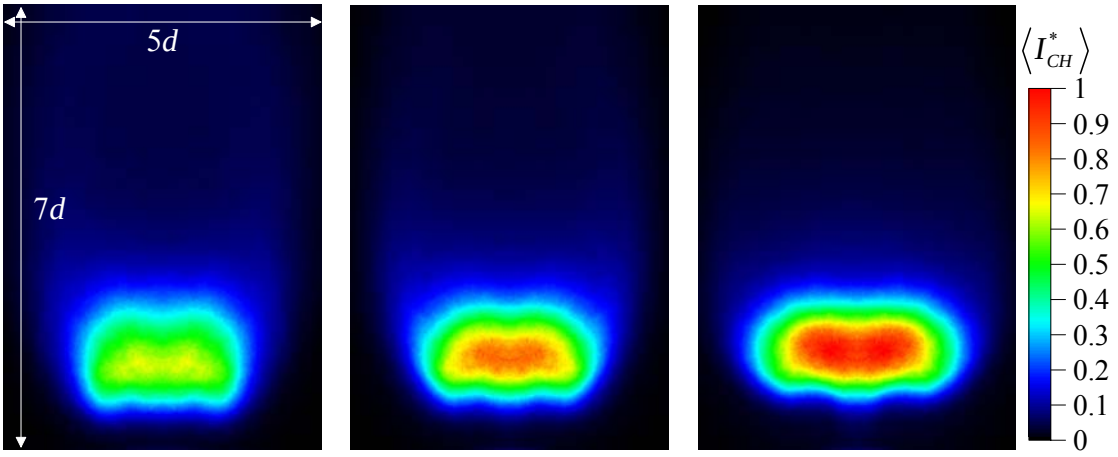

(a) (b) (c)

Figure 3. Time-average distributions of integral CH* chemiluminescence for a lifted strongly swirling flame (a) without periodic forcing and under forcing with St = 0.6: (b) a_f/U_0 = 20%, (c) a_f/U_0 = 30%. S = 1.0, Re_{air} = 4 100, Φ = 2.5, U_0 = 4.7 m/s

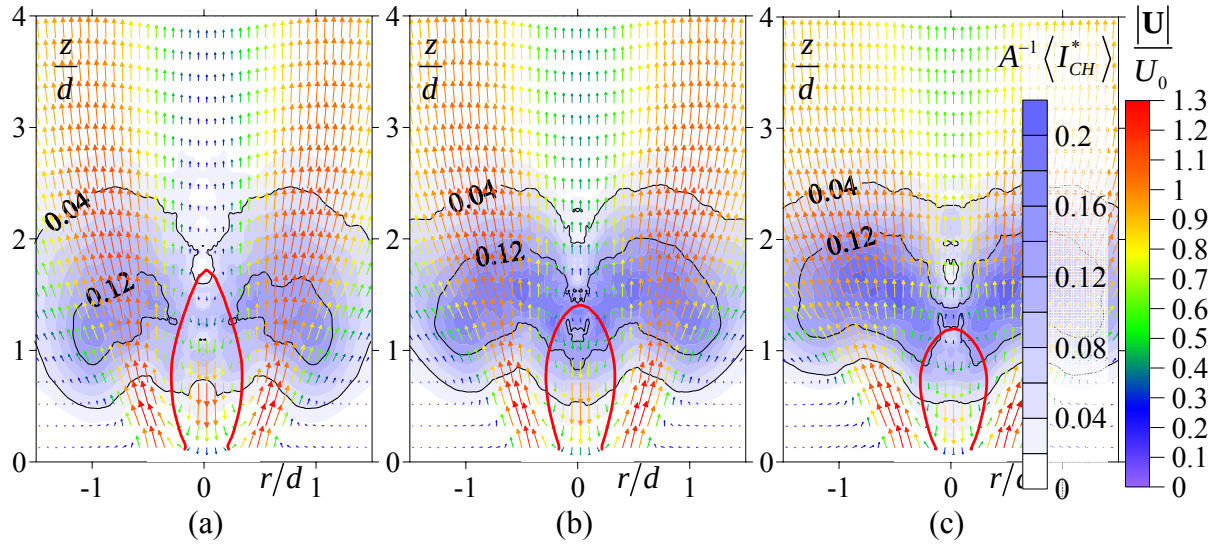

Figure 4. Spatial distributions of the mean velocity and reconstructed CH* chemiluminescence source in the central plane of a lifted strongly swirling flame (a) without periodic forcing and under forcing with St = 0.6: (b) $a_f/U_0 = 20\%$, (c) $a_f/U_0 = 30\%$. $S = 1.0$, $\mathrm{Re}_{air} = 4\,100$, $\Phi = 2.5$, $U_0 = 4.7$ m/s. Red heavy line shows recirculation zone.

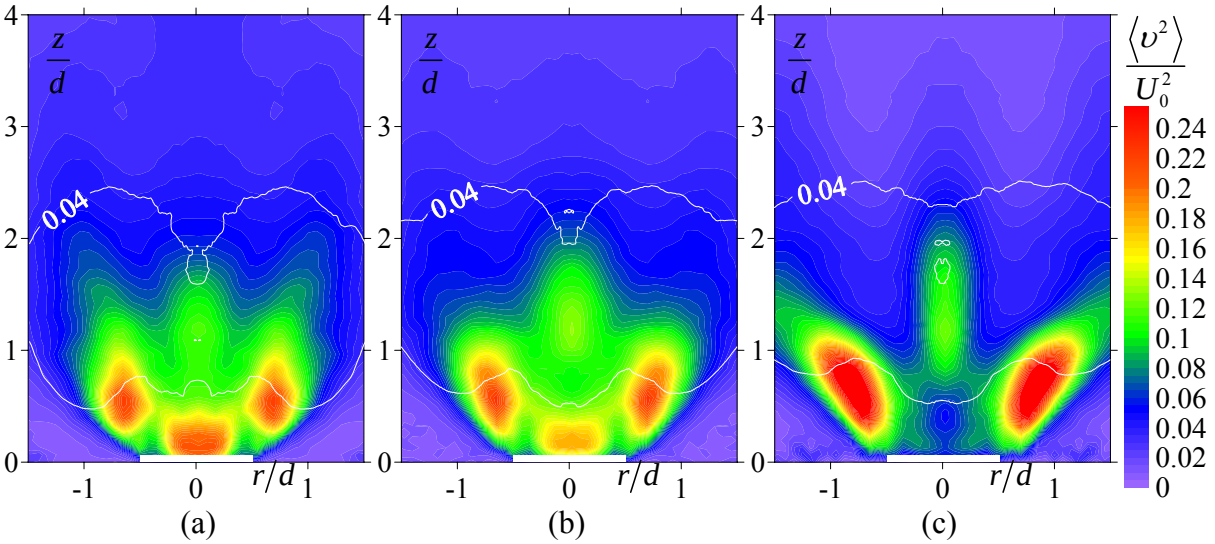

Figure 5. Spatial distributions of the radial component of turbulent kinetic energy for the central plane of a lifted strongly swirling flame (a) without periodic forcing and under forcing with St = 0.6: (b) $a_f/U_0 = 20\%$, (c) $a_f/U_0 = 30\%$. $S = 1.0$, $\mathrm{Re}_{air} = 4\,100$, $\Phi = 2.5$, $U_0 = 4.7$ m/s. White solid line shows iso-level of $A^{-1}\langle I^*_{\mathrm{CH}}\rangle = 0.04$ a.u.

A significant modification in distributions of the radial component of TKE by the forcing can be outlined from Figure 5. The main distinction for the case of $a_f = 30\%$ is that $\langle \upsilon^2 \rangle$ was significantly decreased around the jet axis, near the nozzle exit ($r/d < 0.5$ and $z/d < 0.5$). Similar changes in the distributions of the azimuthal TKE component were detected (not shown in the paper). This indicates that the precession of the flow inside the RZ was suppressed when the forcing with St = 0.6 and $a_f = 30\%$ was applied. The suppression of vortex core precession took place for the reacting flow case only, while for the isothermal flow at the same conditions there was no significant effect.

Figures 6 and 7 shows the difference between the mean velocity fields and magnitude of the radial component of TKE between the reacting and isothermal flows at the same initial

conditions. From Figure 6a it can be seen that the combustion effect for the unforced flow resulted in increase of the fluid velocity up to 80% in magnitude at $z/d = 2$, $r/d = 1.1$ location. Combustion also increased intensity of the back flow inside the RZ and consequently provided a greater width of the main annular flow issuing from the nozzle. Application of the forcing damped the second effect. After the onset of the turbulent combustion domain, magnitude of the velocity difference between the reacting and isothermal flow grew monotonously with the forcing amplitude. As it was mentioned this is expected to be due to an increase of turbulent combustion rate by the forcing.

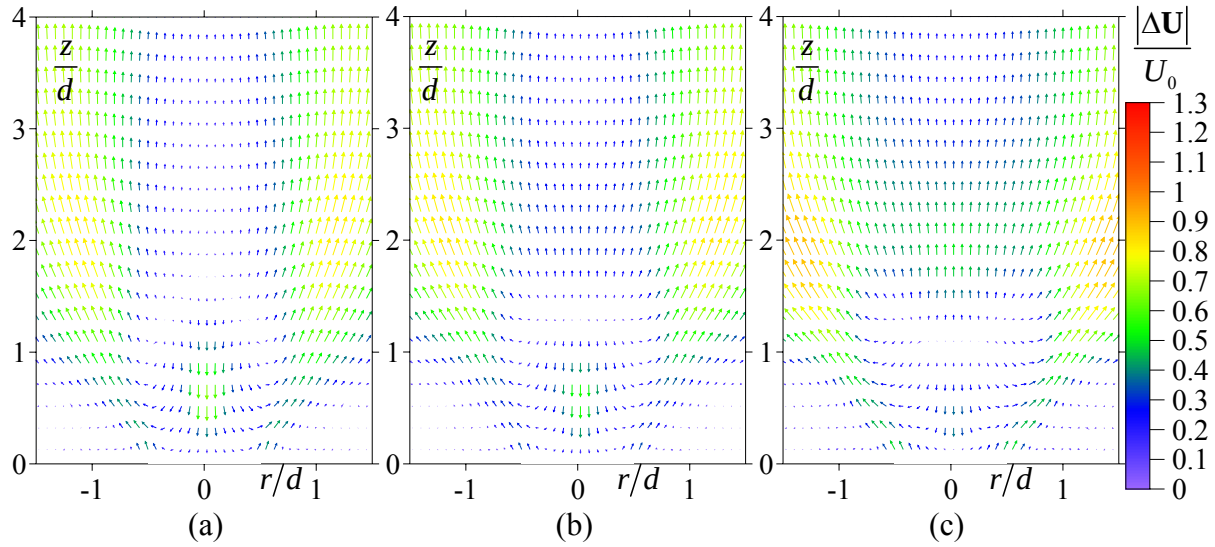

Figure 6. Vector difference of the mean velocity in the central plane of a lifted strongly swirling flame and isothermal jet flow. $S = 1.0$, $\mathrm{Re}_{air} = 4\ 100$, $\Phi = 2.5$, $U_0 = 4.7$ m/s. (a) No external forcing, forcing with St = 0.6: (b) $a_f/U_0 = 20\%$, (c) $a_f/U_0 = 30\%$.

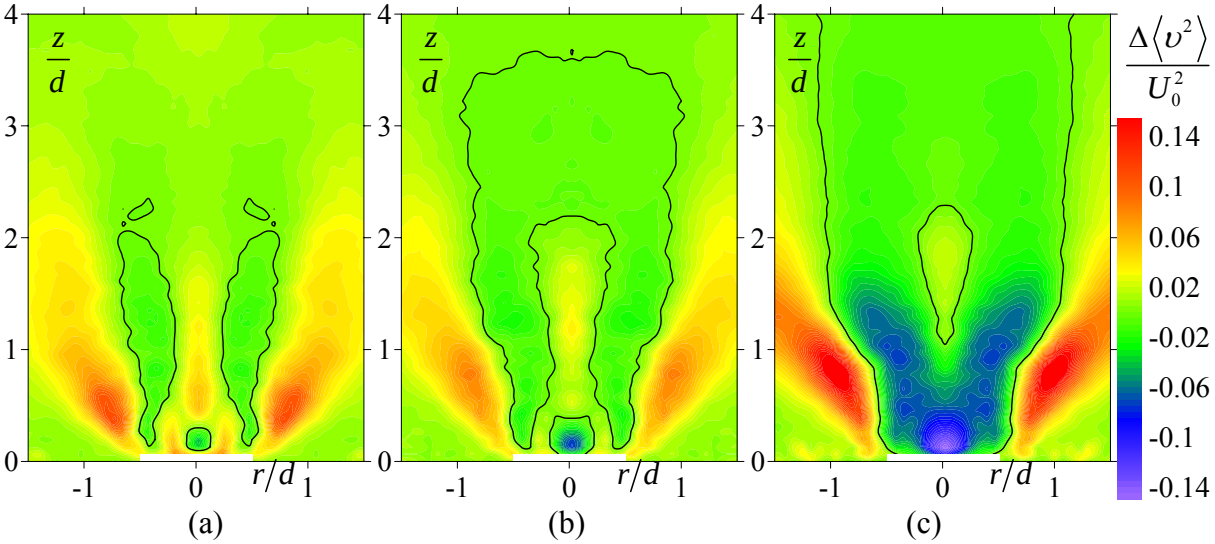

Figure 7. Difference of the radial turbulent kinetic energy in the central plane of a lifted strongly swirling flame and isothermal jet flow. $S = 1.0$, $\mathrm{Re}_{air} = 4\ 100$, $\Phi = 2.5$, $U_0 = 4.7$ m/s. (a) No external forcing, forcing with St = 0.6: (b) $a_f/U_0 = 20\%$, (c) $a_f/U_0 = 30\%$. Black solid line corresponds to $\Delta\langle\upsilon^2\rangle = 0$

The difference between the radial component of TKE for the reacting and isothermal flows is shown Figure 7 for the unforced and forced cases. For the strongly swirling lifted flame without forcing, the combustion increased $\langle\upsilon^2\rangle$ in the outer mixing layer between the

main annular flow coming from the nozzle and the ambient air, where intensive velocity fluctuations were produced by large-scale vortices. This is supposed to be due to an increase of the backflow inside the RZ and a greater spreading of the jet flow owing to the gas expansion. For the case of forcing at $a_f/U_0 = 20\%$ the overall effect of the combustion appears to be similar. In contrast, the application of forcing with $a_f/U_0 = 30\%$ amplitude resulted in substantially different effect on the radial velocity fluctuations near the nozzle exit and jet axis. As seen from Figure 7c, the presence of the lifted flame for the forcing with St = 0.6 and 30% amplitude suppressed significantly the radial velocity fluctuations in the region $r/d < 0.5$ near the nozzle exit, while the velocity pulsation were still intensified in the outer mixing layer $r/d > 0.5$. As speculated in the next section, damping of the radial velocity pulsations in the jet core for the reacting case is expected to be due to the interaction of the ring-like vortices with the lifted flame.

Instantaneous flow patterns

The present section considers the instantaneous structure of the large-scale vortices in the unexcited and forces ($a_f = 30\%$) strongly swirling jets and lifted flames. In general, for the unforced cases (see Figure 8) the instantaneous flow pattern appears to be similar to that of the isothermal strongly swirling jet flow and of the lifted flame for the same nozzle geometry studied in [1] and [3], respectively. The large-scale vortices were formed both in the inner mixing layer (between the main flow and the reverse flow) and in the outer mixing layer (between the main flow and the ambient air). It is expected, that among a band of various modes, a couple of powerful large-scale helices was induced near the stagnation point of the RZ, when the wriggling reverse flow faced the main flow from the nozzle. A similar pattern of the large-scale vortices can be outlined for the lifted non-forced flame, considering the fluid expansion due to the combustion.

Figures 9a and b demonstrate the instantaneous velocity and vorticity fields for the case of the forced ($a_f = 30\%$) isothermal and reacting flows, respectively. This particular example, selected for the isothermal jet demonstrate that the strong forcing induced nearly-symmetrical couples of positive and negative vortices both in the outer and inner mixing layer, while reverse flow still wriggled inside the RZ due to the core precession. Taking into account the relatively large amplitude of the forcing, these couples of the opposite vortices might correspond to vortex rings formed in the mixing layers by the flow pulsing. From the example for the reacting case (Figure 9b), the formation of a similar vortex couple can be seen near the nozzle rim. Another couple located in the outer mixing layer can be also detected after the lifted flame. In contrast to the isothermal flow at the same conditions, the radial velocity fluctuations inside the RZ for $z/d < 1.0$ were rather small. Thus, the suppression of the reverse flow precession is expected to be due to the ring-like vortices interaction with the lifted flame front. It is also supposed, that possible variation of the swirl rate due to the forcing [19], had a minor effect in this case, since the swirl rate of the burner was significantly above of a critical value.

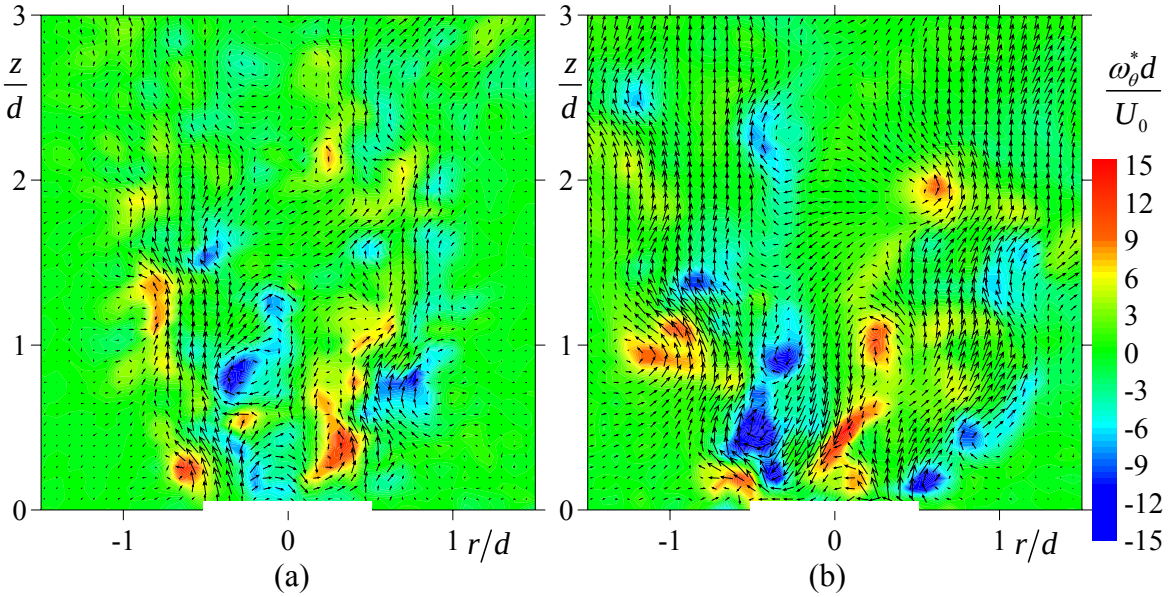

Figure 8. Instantaneous velocity and vorticity fields in the central plane of a strongly swirling (a) isothermal jet and (b) lifted flame without periodic forcing $S = 1.0$, $\mathrm{Re}_{air} = 4\ 100$, $\Phi = 2.5$, $U_0 = 4.7$ m/s.

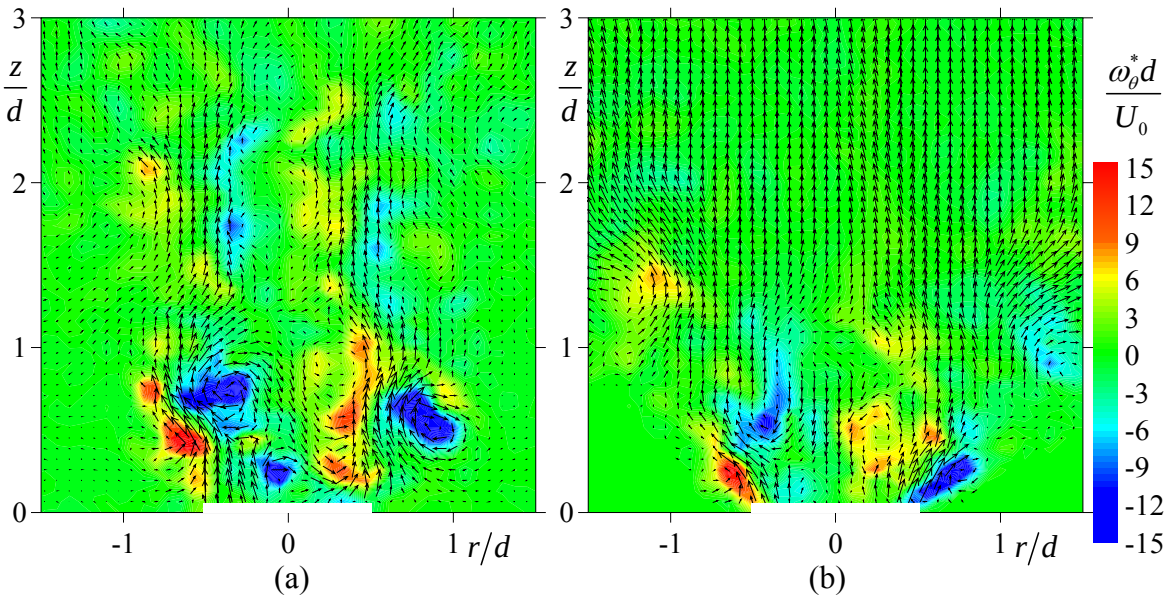

Figure 9. Instantaneous velocity and vorticity fields in the central plane of a strongly swirling (a) isothermal jet and (b) lifted flame and under periodic forcing with St = 0.6 and $a_f/U_0 = 30\%$. $S = 1.0$, $\mathrm{Re}_{air} = 4\ 100$, $\Phi = 2.5$, $U_0 = 4.7$ m/s.

Conclusions

The flow structure of a strongly swirling lifted propane-air turbulent flame under periodical forcing was studied experimentally. Ensembles of the instantaneous velocity fields were measured by means of stereo PIV, and the spatial distributions of the mean velocity and intensity of turbulent fluctuations were calculated. In order to visualise the domain of intensive turbulent combustion, CH* chemiluminescence images were captured by ICCD camera and their average was processed by inverse Abel transform. The results demonstrate the strong axial forcing (with amplitude 30% of U_0) of the lifted strongly swirling flame can provide an increase of combustion rate and suppression of the vortex core precession near the

nozzle exit via forcing the large-scale vortices. By comparison the flow structure of the reacting and isothermal flows under the strong forcing it was observed that significant suppression took place only for the reacting case, indicating that vortices interaction with the lifted flame plays a key role in this effect.

Acknowledgements
The work was fulfilled under foundation by Russian Foundation for Basic Research (grants NN 07-08-00213, 07-08-00710 and 10-08-01304). The work was also partially supported by Federal Oriented Program «Scientific, research and educational cadres for innovative Russia» for 2009-2013.

Nomenclature

A	Abel transform operator
I_{CH}	image intensity of CH* chemiluminescence
Re_{air}	Reynolds number based on air viscosity and flowrate
S	swirl rate
St	Strouhal number
U	mean axial velocity
a_f	forcing amplitude
d	nozzle exit diameter
r	radial coordinate
z	axial coordinate
Φ	equivalence ratio
θ	azimuthal coordinate
υ	fluctuation of the radial velocity
ω	vorticity

Subscripts

0	average value at the nozzle exit for flow without swirl

Superscripts

*	instantaneous quantity

References

[1] Alekseenko, S.V., Dulin, V.M., Kozorezov, Yu.S., Markovich, D.M., "Effect of axisymmetric forcing on structure of a swirling turbulent jet", *Int. J. Heat and Fluid Flow* 29: 1699-1715 (2008).

[2] Alekseenko, S.V., Dulin, V.M., Kozorezov, Yu.S., Markovich, D.M., "Effect of external periodic excitation on a swirling suspended flame", *Tech. Phys. Lett.* 37: 278-281 (2011a).

[3] Alekseenko, S.V., Dulin, V.M., Kozorezov, Yu.S., Markovich, D.M., Shtork, S.I., Tokarev, M.P., "Flow structure of swirling turbulent propane flames", *Flow, Turb. and Comb.* DOI 10.1007/s10494-011-9340-5 (2011b).

[4] Anacleto, P.M., Fernandes, E.C., Heitor, M.V., Shtork, S.I., "Swirl flow structure and flame characteristics in a model lean premixed combustor" *Combust. Sci. Technol.* 175: 1369-1388 (2003).

[5] Broze, G., Hussain, F., "Transitions to chaos in a forced jet: intermittency, tangent bifurcations and hysteresis", *J. Fluid Mech.* 311: 37-71 (1996).

[6] Cala, C.E., Fernandes, E.C., Heitor, M.V., Shtork, S.I., "Coherent structures in unsteady swirling jet flow", *Exp. Fluids* 40: 267-276 (2006).
[7] Chao, Y.C., Yuan, T., Jong, Y.C., "Measurements of the stabilization zone of a lifted jet flame under acoustic excitation" *Exp. Fluids* 17:381-389 (1994).
[8] Cheng, R.K., "Low Swirl Combustion" *The Gas Turbine Handbook*, 2006
[9] Clark, T.P., "Studies of OH, CO, CH, and C2 radiation from laminar and turbulent propane-air and ethylene-air flames" *NACA tech. note* No 4266 (1958)
[10] Gallaire, F., Rott, S., Chomaz, J.-M., "Experimental study of a free and forced swirling jet", *Phys. Fluids* 16:2907-2917 (2004).
[11] Guezennec, Y.G., Brodkey, R.S., Trigui, N., Kent, J.C., "Algorithms for fully automated three-dimensional particle tracking velocimetry", *Exp. Fluids* 17:209-219 (1994).
[12] Iudiciani, P., Duwig, C., "Large eddy simulation of the sensitivity of vortex breakdown and flame stabilisation to axial forcing", *Flow, Turb. and Comb* 86:639–666 (2011).
[13] Konle, M., Kiesewetter, F., Sattelmayer, T., "Simultaneous high repetition rate PIV–LIF-measurements of CIVB driven flashback", *Exp. Fluids* 44:529-538 (2008).
[14] Kurimoto, N., Suzuki, Y., Kasagi, N., "Active control of lifted diffusion flames with arrayed micro actuators" *Exp. Fluids* 39: 995-1008 (2005)
[15] Legrand, M., Nogueira, J., Lecuona, A., Nauri, S., Rodríguez, P.A., "Atmospheric low swirl burner flow characterization with Stereo-PIV" *Exp. Fluids* 48:901-913 (2009)
[16] Liang, H., Maxworthy, T., "Experimental investigations of a swirling jet in both stationary and rotating surroundings", *Exp. Fluids* 45:283-293 (2008).
[17] Lin, C.K., Jeng, M.S., Chao, Y.C. "The stabilization mechanism of the lifted jet diffusion flame in the hysteresis region" *Exp. Fluids* 14: 353-365 (1993).
[18] Mourtazin, D., Cohen, J., "The effect of buoyancy on vortex breakdown in a swirling jet", *J. of Fluid Mech.* 571:177-189 (2007).
[19] Palies, P., Schuller, T., Durox, D., Gicquel, L.Y.M., Candel, S., " Acoustically perturbed turbulent premixed swirling flames", *Phys. Fluids* 23: 037101 (2011)
[20] Ruith, M.R., Chen, P., Meiburg, E., Maxworthy T., "Three-dimensional vortex breakdown in swirling jets and wakes: direct numerical simulation", *J. Fluid Mech.* 486: 331-378 (2003).
[21] Saiki, Y., Suzuki, Y., Kasagi, N., "Active control of swirling coaxial jet mixing with manipulation of large-scale vortical structures" *Flow, Turb. and Comb* DOI 10.1007/s10494-010-9274-3 (2011).
[22] Suzuki, H., Kasagi, N., Suzuki, Y., "Active control of an axisymmetric jet with distributed electromagnetic flap actuators" *Exp. Fluids* 36: 489-509 (2004).
[23] Takehara, K., Etoh, T., "A study on particle identification in PTV. Particle mask correlation method", *J. Visualization* 1:313-323 (1998).
[24] Westerweel, J., Scarano, F., "Universal outlier detection for PIV data", *Exp. Fluids* 39:1096-1100 (2005).